

Measurement of the asymmetry parameter for ^{29}P β decay

G. S. Masson* and P. A. Quin

Department of Physics, University of Wisconsin, Madison, Wisconsin 53706

(Received 28 February 1990)

The asymmetry parameter for the ground state, mirror decay of polarized ^{29}P has been measured. The ^{29}P were produced with the $^{28}\text{Si}(\vec{d},p)$ reaction, and the sample polarization was determined from a simultaneous measurement of the asymmetry for the pure Gamow-Teller transition to the first excited state in ^{29}Si at 1.27 MeV. The result, $A_{\text{g.s.}} = 0.681 \pm 0.086$, is in good agreement with the $V - A$ theory of nuclear β decay.

I. INTRODUCTION

The conserved-vector-current hypothesis (CVC) and isospin invariance require, subject to small corrections, that the product ft of the statistical rate function and the half-life for superallowed Fermi transitions is a universal constant. Although the present situation is not entirely satisfactory (see Wilkinson¹ for a recent review), significant improvements in experimental accuracy^{2,3} and in the treatment of the isospin nonconservation and radiative correction terms³⁻⁶ permit a critical test of CVC and the three-generation standard model.^{1,3-5}

The beta decay between mirror nuclei provides an equally populous sector to which the CVC hypothesis and isospin-invariance constraints apply. Mirror transitions are, in addition, sensitive to a variety of extensions of the usual $V - A$ theory of nuclear beta decay; e.g., the well characterized⁷ but generally unmeasured recoil order terms, as well as exotic extensions of the standard model.^{1,8} An auxiliary measurement is required to determine the Gamow-Teller contribution, and as a consequence only four transitions have been studied to date. Here again recent experiments have improved the accuracy for free-neutron decay^{9,10} and clarified a long-standing anomaly for ^{35}Ar decay.¹¹ The investigation of a wider variety of mirror transitions may be possible with the application of two techniques that lend themselves to the production of polarized mirror nuclei that decay by positron emission. These are the transfer of polarization in reactions initiated by polarized beams, employed in Ref. 11 and this experiment, and the utilization¹² of on-line, low-temperature nuclear orientation.

We report here a measurement of the asymmetry parameter A for ^{29}P decay to the ground state of ^{29}Si . The ^{29}P was produced and polarized using the $^{28}\text{Si}(\vec{d},n)^{29}\text{P}$ reaction initiated with vector polarized deuterons, and the pure Gamow-Teller transition to the first excited state of ^{29}Si was used to determine the nuclear polarization. The formalism required for the analysis of this experiment is given in Sec. II, followed in Secs. III and IV by a description of the experiment and the data analysis procedure. The result is presented and discussed in Sec. V.

II. FORMALISM

The fundamental quantity extracted from measurements of the integrated beta-decay transition probability for superallowed Fermi decays is⁴

$$\mathcal{F}t_{\text{Fermi}} = \frac{K}{G_V'^2 |C_V M_F|^2} = [f(1 + \delta_R)(1 - \delta_C)]t, \quad (1)$$

where K is a product of fundamental constants, G_V' is the vector coupling constant for nucleon decay, C_V is the zero-momentum-vector form factor, M_F is the Fermi matrix element, and δ_R and δ_C are nucleus-dependent radiative and isospin nonconservation corrections to f and $|M_F|^2$, respectively. CVC requires $C_V = 1$ for all transitions, and the simple isospin structure of these transitions gives $|M_F|^2 = [T(T+1) - T_Z T_{Z_f}] \delta_{i,f}^J \delta_{i,f}^T$. Other contributions, such as recoil order terms, possible scalar current contributions, etc., are known^{3,13} to be small. Hence, for isospin $T=1$ and the corrected $|C_V M_F|^2 \equiv 2$, the CVC aspect of the standard model predicts that $\mathcal{F}t_{\text{Fermi}}$ is a universal constant. Recent analyses^{1,3,4} verify Eq. (1) at the level of $\pm 0.04\%$, although there is an approximately $\pm 0.1\%$ systematic uncertainty in the evaluation^{3,4} of δ_C .

The axial-vector (Gamow-Teller) contribution to the transition rate must be included in Eq. (1) when $T = \frac{1}{2}$ mirror decays are considered. With this additional term, written as a ratio of the Gamow-Teller and Fermi form factors and matrix elements $\rho = C_A M_{\text{GT}} / C_V M_F$, Eq. (1) generalizes to

$$(1 + \rho^2) \mathcal{F}t_{\text{mirror}} = \frac{K}{G_V'^2 |C_V M_F|^2} = (1 + \rho^2) [f_v(1 + \delta_R)(1 - \delta_C)]t, \quad (2)$$

where f_v is the vector statistical rate function.¹⁴ Since here $|C_V M_F|^2 \equiv 1$, Eqs. (1) and (2) can be combined into the simple relation

$$(1 + \rho^2) \mathcal{F}t_{\text{mirror}} = 2 \mathcal{F}t_{\text{Fermi}}. \quad (3)$$

Unfortunately $C_A M_{\text{GT}}$ is not simply calculated, and a

test for equality in Eq. (3) requires that ρ be obtained from an auxiliary measurement. An alternative approach is to use Eq. (3) as the defining equation for ρ and then predict other observables, such as the asymmetry parameter for polarized nucleus beta decay, which can then be compared with experiment.

The measurement of A exploits the angular dependence of the transition rate for allowed nuclear beta decay,⁷ viz.,

$$W(\theta) = W_0 \left[1 + \frac{v}{c} P A \cos(\theta) \right], \quad (4)$$

where $v(c)$ is the speed of the positron (light), P is the nuclear polarization, and θ is the angle between \mathbf{v} and \mathbf{P} . Using detectors at $\theta=0$ and π in combination with reversal of the nuclear polarization ($\pm P$), an asymmetry

$$\mathcal{A} = \langle P \rangle_{\theta, v/c} A = \frac{R-1}{R+1}, \quad (5)$$

is measured, where

$$R = \left[\frac{N(0, +P)N(\pi, -P)}{N(0, -P)N(\pi, +P)} \right]^{1/2}. \quad (6)$$

Here $\langle P \rangle_{\theta, v/c}$ denotes the averaging over the angular acceptance of the detectors and the phase space distribution of the beta spectrum, and $N(\theta, \pm P)$ is the number of counts observed for each detector-polarization combination. The asymmetry parameter A can only be obtained from the asymmetry \mathcal{A} if the nuclear polarization $\langle P \rangle_{\theta, v/c}$ is known. In the present experiment the dependence on the nuclear polarization is removed by simultaneously measuring the asymmetry \mathcal{A}_{ex} for the pure Gamow-Teller transition to the first excited state in ^{29}P at 1.27 MeV. The asymmetry parameter for this transition is known from angular momentum coupling alone. This technique, which has also been used^{11,15} for ^{35}Ar , relies on the fact that the decay to the excited state can be isolated by coincidences with a subsequent decay γ ray. After experimental corrections to the ground-state and excited-state asymmetries, it is the ratio $\mathcal{A}_{\text{g.s.}}/\mathcal{A}_{\text{ex}}$ that is directly measured in the experiment.

In the $V-A$ approximation the asymmetry parameters for the ^{29}P ground state, $J=\frac{1}{2}$, mirror transition and pure Gamow-Teller $J=\frac{1}{2} \rightarrow J=\frac{3}{2}$ excited-state transition can be written⁷

$$A_{\text{g.s.}} = \frac{2}{3} \left[\frac{\rho^2 - \sqrt{3}\rho}{1 + \rho^2} \right], \quad (7)$$

and $A_{\text{ex}} = -\frac{1}{3}$. Previous analyses^{11,16} for ^{35}Ar decay have used the measured asymmetry parameter and ft value in Eqs. (2) and (7) to eliminate ρ and obtain the quark mixing (Cabibbo) angle θ_1 , where $G_V' = \cos(\theta_1)G_V$. This procedure has the disadvantage that the resultant error on θ_1 [or, for that matter, on $G_V'^2$ in Eq. (2)] is nonlinear, and moreover the contribution of systematic effects in the asymmetry parameter measurement is difficult to discern. In this work Eq. (3) is evaluated to obtain ρ , with the sign of ρ given by shell-model calcula-

tions or magnetic-moment systematics,¹⁷ and then Eq. (7) gives the mirror transition asymmetry parameter $A_{\text{g.s.}} \equiv A_{\mathcal{J}T}$. Since A_{ex} is known, the ratio $A_{\mathcal{J}T}/A_{\text{ex}}$, which typically has small statistical and systematic uncertainties and a linear error structure, is compared to the experimental result $\mathcal{A}_{\text{g.s.}}/\mathcal{A}_{\text{ex}}$. The essential point is that contributions outside of $V-A$ will in general lead to a violation of the equality

$$\left(\frac{A_{\text{ex}}}{A_{\mathcal{J}T}} \right) \left(\frac{\mathcal{A}_{\text{g.s.}}}{\mathcal{A}_{\text{ex}}} \right) = 1. \quad (8)$$

III. EXPERIMENTAL DETAILS

Polarized ^{29}P was produced using the $^{28}\text{Si}(\vec{d}, ^2\vec{P})n$ reaction. Vector-polarized deuterons from a polarized-ion source¹⁸ were accelerated by a tandem accelerator, momentum analyzed, and focused on the target, a $1.0 \times 1.0 \times 0.035 \text{ cm}^3$ crystal wafer of high-purity, natural isotopic abundance silicon oriented at 45° relative to the beam direction and to the beta detectors. A tantalum collimator with a 1.6-mm-diameter aperture, placed 25-cm upstream from the target, defined the beam spot on target and intercepted approximately 0.05% of the total beam current. The beam current on the target was limited to 20 nA by detector gain stability, accidental rate, and pile-up rate considerations.

The detector apparatus is shown schematically in Fig. 1. Positrons emitted by the target passed through 25- μm Kapton windows were detected in two, three-element telescopes placed above and below the target chamber. The first two elements, 1-mm-thick plastic scintillators ΔE_1 and ΔE_2 , defined the acceptance of the telescopes;

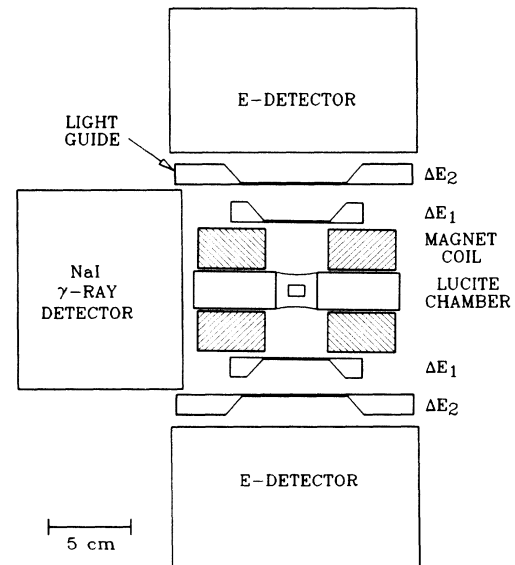


FIG. 1. Diagram of the target and detector apparatus used for the experiment. The beta detectors have cylindrical symmetry about a vertical axis through their center. The soft iron flux return for the magnet and lead shielding for the NaI γ -ray detector are not shown.

viewed from the target, each telescope subtended a solid angle of 0.66 sr. The third element was the E detector, a 15-cm-diameter \times 9-cm-thick plastic scintillator, which stopped the positrons and measured their energy. Each scintillator was coupled to a photomultiplier tube with a light guide. An 11.4-cm-diameter \times 10.7-cm-thick NaI crystal, placed 6.3 cm from the target and shielded from positrons by 5 cm of lucite, was used to detect γ rays. Two magnet coils, used to produce a vertical polarization-holding field at the target, partially obstructed the NaI detector and reduced its effective solid angle to 0.55 sr. Anode signals from photomultiplier tubes were split and used as inputs to charge integrating analog-to-digital converters (ADC) to provide pulse-height information and as inputs to constant-fraction discriminators to provide timing information.

The experiment was conducted in the following fashion. The target was first activated for 4 s, the nominal half-life¹⁹ of ^{29}P , during which time the photomultiplier tube cathodes were positively biased to reduce their gain. The beam was then deflected from the target, the photocathodes were grounded, and the detectors allowed to stabilize for 250 ms. Data were then recorded in three time intervals of 2, 2, and 4 s, to monitor the sample polarization relaxation time and half-life. The beam polarization was then reversed and the cycle repeated.

Timing signals from the ΔE_1 and ΔE_2 detectors of a telescope were put into a coincidence circuit with a resolving time of 90 ns to form a β -event signal. A second coincidence circuit, with a resolving time of 160 ns, was used to generate $\beta\gamma$ -event signals from the β -event signal and the NaI detector timing signal. The NaI detector electronics included a pileup detection circuit to identify events where two γ -ray timing signals occurred between 170 ns and 1.0 μs of each other. Typical β - and $\beta\gamma$ -event rates were 40 kHz and 100 Hz, respectively. The β events were scaled by 100 to reduce the acquisition system dead time. These scaled β -event signals and $\beta\gamma$ -event signals were combined to form an ADC gate, a time-to-digital converter start signal, and a computer interrupt. For each event the computer recorded the following information, which was subsequently archived on

tape: the pulse height in the ΔE_1 , ΔE_2 , E , and NaI detectors, the relative timing between the ΔE_1 detector and the ΔE_2 , E , and NaI detectors, and a series of flags indicating the deuteron beam polarization direction, the telescope, counting interval within a cycle, β or $\beta\gamma$ event, and the NaI pileup detector status (TRUE or FALSE). The information obtained from the NaI detector was not used in the analysis of the β events, but was acquired to maintain equal computer dead times for β and $\beta\gamma$ events.

The beam energy, target temperature, and strength of the magnetic-holding field were varied to maximize the polarization of the ^{29}P sample. Figure 2 shows the measured ground-state asymmetry, which is proportional to the ^{29}P polarization, as a function of these parameters and of the time after activation. The arrows in panels A–C indicate the parameter values chosen for the experiment and also the value used in the other panels. The arrow in the panel D indicates that the data in panels A–C were measured during the 2 s counting interval immediately following activation. The maximum polarization transfer coefficient and relaxation time,²⁰ $K_y^{\beta} \approx 0.084 \pm 0.001$ and $T_1 = 11.2 \pm 0.6$ s, respectively, and deuteron beam vector polarization $p = 0.60 \pm 0.01$ give a nuclear polarization $P \approx 0.075$ at the time of ^{29}P formation and an average (including the contribution of previous cycles) polarization of 0.038 over the 8 s counting period. The ground-state asymmetry was observed to decrease about 15% per day, the most likely cause being radiation damage to the target that results in a decrease in T_1 . The data in Fig. 2, taken at different times, exhibit this effect. The target was replaced about once a day to reduce this polarization loss.

IV. DATA ANALYSIS

A. General remarks

A total of 2×10^{10} events were observed during three running periods, with about 3×10^8 events archived to tape. Data were sorted by telescope, polarization direction, and counting interval into energy and timing spectra. After applying constraints or “cuts” and correc-

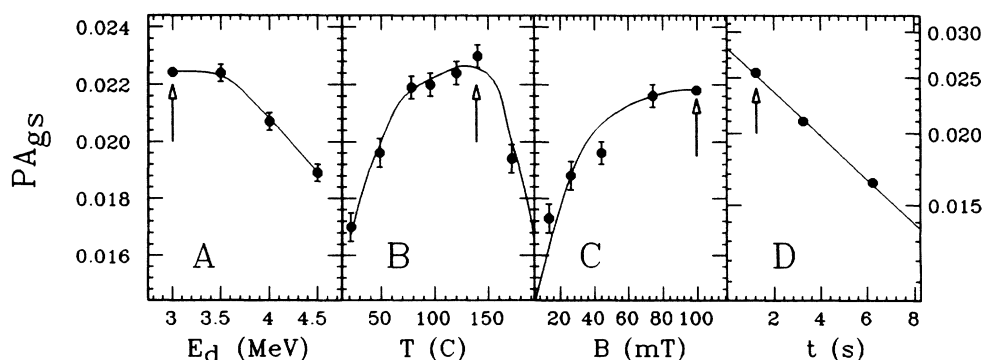


FIG. 2. The ^{29}P ground-state asymmetry, P_{Ags} , is shown as a function of the deuteron bombarding energy, target temperature, magnitude of the external holding field, and time after activation in panels A–D, respectively. The curves shown in panels A–C are guides for the eye only, and the arrows indicate the values chosen for the asymmetry measurement. The data in these panels is from the first 2 s measuring interval after activation, as indicated by the arrow in panel D. The straight line in panel D is an exponential fit which gives a polarization relaxation time $T_1 = 11.2 \pm 0.6$ s. See the text for details on the polarization and the transfer coefficient K_y^{β} .

tions, these spectra were analyzed to obtain the asymmetries for the ground- and first excited-state transitions in the decay of ^{29}P .

Three cuts were applied to all events. A minimum pulse height was required in both the ΔE_1 and ΔE_2 detectors. These two cuts removed most events where the positron passed through a light guide, with the emission of Čerenkov radiation, rather than through the scintillator. The residual light guide event contribution to the ΔE_1 and ΔE_2 detector spectra was $\lesssim 0.5\%$ and $\lesssim 2\%$, respectively (see Sec. IV D). Accepted events were also required to have relative ΔE_1 - ΔE_2 timing within a 6 ns cut centered on the 1.5-ns full width at half maximum (FWHM) “true” coincidence peak. The accidental contribution within the timing cut was $< 0.15\%$.

B. Ground-state transition

Figure 3 shows a β -event E detector pulse-height spectrum for a small portion of the events (but typical of the size into which the events were binned to study short-term systematic effects) obtained using the cuts described above. The peak in the spectrum at about 0.3 MeV results from events where a positron generates a ΔE_1 - ΔE_2 coincidence, stops and annihilates before reaching the E detector, with one of the resulting 511-keV photons Compton scattering in the E detector. The shape of the peak results from summing the relatively flat Compton scattering distribution and the positron phase-space distribution. This explanation was confirmed by observing coincidences between one telescope and the opposite E

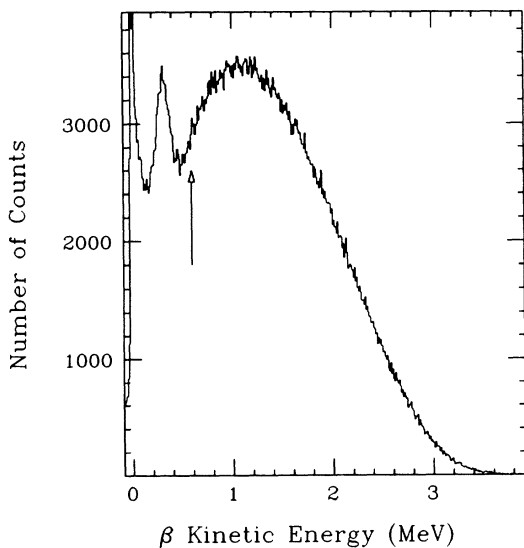


FIG. 3. An E beta detector pulse-height spectrum typical of the size used to search for short-term systematic effects is shown. This spectrum is for the first 2 s counting interval, and it corresponds to $\approx 0.25\%$ of the events archived to tape. The peak at about 0.3-MeV results from Compton scattering of 511-keV γ rays (see the text for details). A software cut at 0.6-MeV beta kinetic energy, indicated by the arrow, was applied prior to the analysis of the NaI γ -ray events, and also prior to extracting the ground-state asymmetry.

detector, with the first telescope serving as the source of the annihilation radiation. The complex, low-energy portion of the spectrum was excluded by cutting the E detector spectra to include only those events above the arrow shown in Fig. 3. This threshold corresponds to an energy deposited in the E detector of approximately 600 keV, or a total beta kinetic energy of ≈ 1.1 MeV. After this cut was applied, the accidental contribution to the E detector spectra, within an 8 ns cut centered on the 2.2-ns FWHM “true” coincidence peak, was $< 0.05\%$.

Several beta emitters, produced by (d,n) , (d,p) , and (d,α) reactions on the natural silicon target, contribute to the E detector spectrum. The contributions of ^{29}P , $^{26}\text{Al}^m$, ^{28}Al , and ^{30}P were deduced from the $\beta\gamma$ -event spectra and from a separate measurement of the decay rate during a 60 s interval following a 4 s activation. A constant background, consistent with the decay of ^{31}Si ($t_{1/2} = 2.6$ h), was also observed. No evidence was found for reaction products from possible carbon or oxygen contaminants in the target.

Of the four identified contributions to the E detector spectrum, only ^{29}P is expected to exhibit an asymmetry for the following reasons. First, the half-lives of ^{28}Al and ^{30}P are much longer than the 12.25 s spin-reversal cycle time. As a consequence, averaging over many spin-reversal cycles leads to a reduction in the asymmetry by a multiplicative factor ϵ which is typically small; e.g., $\epsilon = 0.01$ or 0.03 for polarization relaxation times of 12.25 s or infinity, respectively. Analysis of the $\beta\gamma$ events gave zero asymmetry within statistics for ^{28}Al , and the same result is assumed true for ^{30}P . Second, $^{26}\text{Al}^m$ has spin $J = 0$, and the asymmetry identically vanishes. Thus the reduction in the E detector asymmetry is simply given by the fractional contribution of ^{29}P to the integral of the E detector pulse-height distribution. Summed over the 8 s counting interval and the pulse-height cut shown in Fig. 3, the ^{29}P contribution is 0.908 ± 0.008 . To obtain the asymmetry for the ^{29}P ground-state transition, the β -event asymmetry must be further increased by $(0.7 \pm 0.01)\%$ to account for the 1.2% ^{29}P branches to the excited states in ^{29}Si . This last correction was calculated using the known excited-state branching ratios,¹⁹ which gives an excited-state contribution of 0.44% of the β events above the E detector cut, and the final excited-state asymmetry \mathcal{A}_{ex} measured in the present experiment.

C. Excited-state transition

1. The γ -ray spectrum

The asymmetry for the 1.1% ^{29}P branch to the 1.27-MeV first excited state in ^{29}Si was obtained from the NaI detector photopeak γ -ray intensities measured in coincidence with the β events. A coincident NaI γ -ray spectrum with only the ΔE_1 and ΔE_2 cuts described in Sec. IV A is shown in Fig. 4. Here again the sample size is typical of the binning used to search for short-term systematic effects. The threshold of the NaI discriminator was set (as indicated by the arrow in Fig. 4) at 700-keV γ -ray energy, slightly above the dominant 511-keV annihilation radiation contribution to the β - γ coincidences. The events appearing below this threshold are a mini-

cule fraction of the potential number of events in this pulse-height region, and these events arise as an artifact of the rise-time dependence of the NaI discriminator threshold. These subthreshold events also suffer a pulse-height distortion due to the narrow, 120-ns width of the ADC gate. The peaks in Fig. 4 labeled *A* and *C* correspond to the ^{29}P transition to the first and third excited states in ^{29}Si at 1.27 and 2.43 MeV, respectively. Peak *B* is from ^{28}Al decay to the first excited state of ^{28}Si at 1.78 MeV (a 100% branch). Including the *E* detector pulse-height cut (see Sec. IV B) removed most events for decay to the 2.43-MeV state, as shown in Fig. 5 panel *A*, and this branch was not included in the analysis. This figure also shows that the γ -ray spectra were cut to exclude events with low γ -ray energies, leading to a considerable improvement in the true coincidence peak shape in the β -event–NaI timing spectra. There is significant background under the 1.27-MeV photopeak arising from accidental and pileup events, positron annihilation in flight, and Compton scattering of the 1.78-MeV γ ray from ^{28}Al decay. We discuss each of these backgrounds in turn.

2. Accidental and pileup event corrections

All acceptable $\beta\gamma$ events were required to have relative β -event–NaI timing within a 12 ns cut centered on the 2.6-ns FWHM “true” coincidence peak and a FALSE

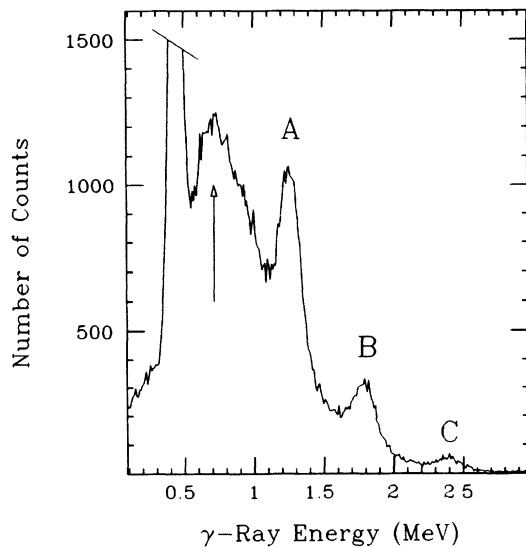


FIG. 4. NaI γ -ray detector pulse-height spectrum typical of the size used to search for short-term systematic effects (this spectrum is from the first 2 s counting interval, and it corresponds to $\approx 0.25\%$ of the events archived to tape). No cuts were applied to the beta *E* detector pulse-height spectrum or to the coincidence timing spectrum. The 700-keV NaI discriminator threshold is indicated by the arrow, and the subthreshold events arise as an artifact of the rise-time dependence of the discriminator. The peaks labeled *A* and *C* correspond to the decay of ^{29}P to the 1.27- and 2.43-MeV levels in ^{29}Si , respectively. Peak *B* is from ^{28}Al decay to the first excited state in ^{28}Si at 1.78 MeV.

signal from the NaI pileup detection circuit. This requirement reduced the accidental events in the *E* detector spectra to $< 0.01\%$. The accidental contribution to the 1.27 and 1.78 photopeaks in the NaI spectra was larger, $\approx 2.5\%$ and 1% , respectively. The accidental NaI energy spectra were determined in the usual way, by placing a cut on the flat accidental background adjacent to the “true” coincidence peak in the β -event–NaI timing spectra. The accidental spectra were then subtracted from the accepted $\beta\gamma$ -event–NaI spectra.

A separate NaI discriminator with the threshold set at 250-keV γ -ray energy was used as the input to the NaI pileup detection circuit. Since the measured pileup detection efficiency was $(87.8 \pm 1.7)\%$, 12.2% of the “true” coincidence events with a TRUE signal from the NaI pileup detector was subtracted from the accepted NaI spectra. This amounted to $\approx 1\%$ of the integrated counts for the 1.27 and 1.78 MeV photopeaks. The combined, normalized accidental and pileup spectrum corresponding to the events shown in Fig. 5 panel *A* is shown in Fig. 5 panel *B*.

3. Positron annihilation in-flight contribution

A fraction of positrons emitted from the target annihilate in flight. The kinematically favored outcome of such an annihilation is to produce two photons, where one receives the bulk of the total available energy and is emit-

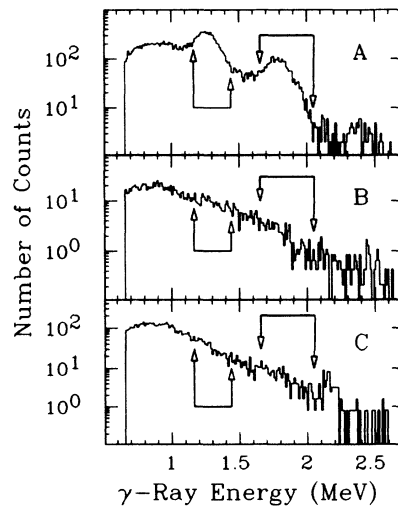


FIG. 5. The NaI γ -ray spectra shown here correspond to events where the beta energy deposited in the *E* detector is above the software cut shown in Fig. 3, and a software cut for the NaI spectrum at $E_\gamma = 0.65$ MEV has also been introduced. The regions used for the analysis of the 1.27-MeV γ ray from ^{29}P decay and 1.78-MeV γ ray from ^{28}Al decay indicated by joined arrows. Panel *A* shows the events corresponding to the “true” coincidence peak in the $\beta\gamma$ -event timing spectrum measured during the first 2 s counting interval. Panel *B* is the normalized accidental and pileup event contribution that must be subtracted from the events in panel *A*. Finally, panel *C* shows the normalized annihilation in flight spectrum obtained from a separate experiment using ^{27}Si decay. This contribution was also subtracted from the events in panel *A*.

ted in a forward direction relative to the positron's momentum. Events of this type give rise to a γ -ray background which has an asymmetry nearly equal to that of the ^{29}P ground state. Because the ground-state asymmetry is opposite in sign and about a factor of 2 larger than the 1.27-MeV γ -ray asymmetry, it is essential to accurately subtract this background.

The decay of ^{27}Si , produced with the $^{27}\text{Al}(p,n)$ reaction, was used to measure the annihilation-in-flight (AIF) background. This is an allowed, positron transition with an end-point energy of 3.85 MeV, $t_{1/2}=4.2$ s, and no excited-state branches.¹⁹ Thus, excepting the 100-keV difference in end-point energy, the β - and γ -ray spectra are identical to those produced by the ^{29}P ground-state decay. The number of events in the cut, β -event, E detector spectra was used to normalize the ^{27}Si AIF $\beta\gamma$ -event NaI spectra to the $\text{Si}(d,n)$ $\beta\gamma$ -event NaI spectra. The E detector pulse-height gains and cuts were sufficiently well matched that this normalization was accurate to within 1%. Differences in dead time for the two experiments were also included. This normalization procedure automatically takes into account the asymmetry of the β -events, which are the source of the AIF background. The AIF background was $\approx 10\%$ and 7% for the 1.27 and 1.78 MeV photopeaks, respectively. The AIF contribution to the events in Fig. 5 panel *A* is shown in Fig. 5 panel *C*. Aside from the slight enhancement near the AIR end point, which arises from an unidentified weak contaminant, the shape of the AIF spectrum agrees with earlier work.²¹

Although a ^{29}P measurement was performed immediately prior to the $\text{Al}(p,n)$ experiment to calibrate the γ -ray energy scale, the uncertainty of this calibration led us to assign an additional $\pm 12\%$ systematic error to the AIF background subtraction. Finally, the effect of the difference in the ^{29}P and ^{27}Si end-point energies was investigated. To do this, the ^{27}Si experiment was repeated with a 0.25-mm aluminum sheet (≈ 100 -keV thick for 2 MeV positrons) placed between the ΔE_1 and ΔE_2 detectors of each telescope. A comparison of the two ^{27}Si experiments showed no statistically significant difference in either the shape or intensity of the AIF spectrum. Moreover, this result implies the AIF background is insensitive to the orientation of the silicon target, which is 120-keV thick for 2-MeV positrons.

4. Contribution from ^{28}Al

The ^{28}Al contribution to the $\beta\gamma$ -event–NaI spectrum is produced by the $^{30}\text{Si}(d,\alpha)$ reaction on the natural silicon target. As discussed previously, the asymmetry for the ^{28}Al decay, averaged over repetitive 12.25 s spin-reversal cycles, was measured to be zero. Compton scattering of 1.78-MeV γ -rays from this decay in the NaI detector contributes a $\approx 23\%$ background under 1.27-MeV photopeak. This background contribution was measured in the following way. An aluminum target was periodically substituted for the silicon target in order to produce a pure ^{28}Al sample with the $^{27}\text{Al}(d,p)$ reaction. The γ -ray spectra was used to accurately determine the ratio of 1.78-MeV γ -ray counts in the 1.27-MeV photo-

peak region to the number of counts in the 1.78-MeV photopeak. Finally, this ratio, typically 0.399 ± 0.002 , and the number of counts in the 1.78-MeV photopeak in spectra such as Fig. 4 peak *A*, were used to subtract the ^{28}Al background. In addition to the statistical error in the number of counts in the 1.78-MeV photopeak, two other uncertainties enter into this subtraction. The first of these arises from background under the 1.78-MeV photopeak in the silicon target spectra. This background is mainly due to ^{29}P decays to the 2.43-MeV level in ^{29}Si and to the simultaneous detection of 1.27- and 0.511-MeV (positron annihilation) γ rays. Fortunately, this background is small ($< 3\%$) and has the same asymmetry as the 1.27-MeV γ rays. This background was ignored, with the consequence that the statistical error in the asymmetry of the 1.27-MeV transition is slightly increased. The second uncertainty is a possible systematic error in choosing the cuts for the 1.78-MeV photopeak. A study of this uncertainty led us to assign a 5% systematic error to the ^{28}Al background subtraction.

5. The low-energy γ -ray spectrum

Prior to the cuts and background subtractions described above, the asymmetry of the ^{29}P γ -ray spectrum adjacent to, but lower in energy than, the 1.27-MeV photopeak was larger in magnitude and opposite in sign to the asymmetry of the photopeak itself, indicating a large fraction of the events were associated with the ground-state decay. After performing all cuts and corrections, the asymmetries of these two regions agreed within errors. However, because of the relatively large background subtractions required and the poor statistical accuracy achieved, the lower-energy portion of the γ -ray spectrum was not included in the calculations of the excited-state transition asymmetry.

D. Sources of false asymmetry and systematic uncertainties

The measurement of asymmetries using a symmetric (up-down) detector arrangement and common data processing electronics cancels or makes negligibly small some corrections and sources of systematic uncertainty. These include detector solid angle effects, spin-dependent beam current modulations, and differences in dead time correlated with spin reversal. However, detector gain shifts correlated with deuteron spin reversal will generate a false asymmetry. No such shifts were observed, and this sets conservative upper limits of $\pm 1 \times 10^{-4}$ and $\pm 2 \times 10^{-4}$ for ground-state and first excited-state asymmetries, respectively. Likewise the $\approx \pm 1 \mu\text{m}$ spin-correlated beam motion measured²² for our polarized-ion source and tandem accelerator could produce a false asymmetry of at most $\lesssim \pm 10^{-5}$ in our experiment. This false asymmetry does not cancel in the asymmetry ratio [Eq. (9)] because the ground-state and first excited-state asymmetries have opposite signs. No dependence on target orientation or magnetic-holding field direction is expected, and none was observed.

Three additional contributions which may affect the ratio $\mathcal{A}_{g.s.}/\mathcal{A}_{ex}$ were investigated. First, the scattering of positrons prior to entering a detector, or scattering out

TABLE I. Systematic uncertainties in $\mathcal{A}_{g.s.}/\mathcal{A}_{ex}$ associated with background subtractions in the $\beta\gamma$ -event-NaI γ -ray spectra, with possible sources of false asymmetries, with averaging $\cos(\theta)$ over the beta detector solid angle, and with averaging v/c over the beta spectrum. See Secs. IV C and IV D for details.

Systematic contribution	Uncertainty in $\mathcal{A}_{g.s.}/\mathcal{A}_{ex}$
Annihilation in flight subtraction	± 0.102
^{28}Al subtraction	± 0.021
β detector gain shifts	± 0.032
Spin-correlated beam motion	± 0.008
Positron scattering	± 0.010
$\langle \cos(\theta) \rangle$	± 0.002
$\langle v/c \rangle$	± 0.001
Total systematic uncertainty	± 0.110

of a telescope without depositing the full energy, distorts the pulse-height spectrum and typically reduces the measured asymmetry. The measured backscattering contribution from a thick sheet of steel placed behind one ΔE_1 detector into the opposite telescope was $(0.07 \pm 0.01)\%$ of the total number of events. A simple modeling of the apparatus gave the result that $(0.5 \pm 0.2)\%$ of the positrons above the E detector threshold were first scattered in the target, or from the target chamber, detectors, or holding field magnet. Such a contribution would reduce the asymmetries by $< 1\%$, and the ratio $\mathcal{A}_{g.s.}/\mathcal{A}_{ex}$ is quite insensitive to this reduction if the energy dependence of the scattering, above our nominal 1-MeV threshold, is not too large. A factor of two difference in the reduction of the asymmetries for the ground state and 1.27-MeV transitions due to positron scattering produces at most a 0.01 difference on the ratio $\mathcal{A}_{g.s.}/\mathcal{A}_{ex}$, and a systematic uncertainty of this size is included in the error calculation. Second, multiple scattering of the positrons, principally in the ΔE_1 detector, changes the effective solid angle for the ground- and first excited-state transitions (this multiple scattering also contributes to the difference in the fraction of light guide events in the ΔE_1 and ΔE_2 spectra). A numerical integration over the ground- and first excited-state energy distributions showed the effect is small, < 20 mrad difference in the effective cone half-angle, and produces a systematic error of < 0.002 in the ratio $\mathcal{A}_{g.s.}/\mathcal{A}_{ex}$. Finally, the uncertainty in the E detector cut shown in Fig. 3 produces an uncertainty in the average value of v/c integrated over the beta spectrum.

TABLE II. Evolution of the cut beta-spectrum asymmetry as corrections are made to obtain $\mathcal{A}_{g.s.}$ for ^{29}P decay to the ground state of ^{29}Si . These data are from the fourth measurement, and are averaged over the 8 s measuring interval (panel D of Fig. 2 shows the time dependence of the cut β -event asymmetry). The final results are corrected for averaging $\cos(\theta)$ over the beta detector solid angle and v/c over the beta spectrum using the cut shown in Fig. 3.

Beta-detector spectrum	Percent of the events	Measured asymmetry $\times 100$	Corrected asymmetry $\times 100$
Cut β events	100	2.10 ± 0.01	
$^{26}\text{Al}^m$, ^{28}Al , ^{30}P , and ^{31}Si	9.20 ± 0.80	0.00 ± 0.20	2.29 ± 0.01
^{29}Si excited states	0.40 ± 0.01	-0.86 ± 0.18	2.31 ± 0.02
Final result	90.40 ± 0.80		2.50 ± 0.02

Again, the ratio $\mathcal{A}_{g.s.}/\mathcal{A}_{ex}$ is quite insensitive to this uncertainty, with a resultant systematic error of only 0.001. The final results are corrected for averaging $\cos(\theta)$ over the beta detector solid angle and v/c over the beta spectra using the cut shown in Fig. 2. These corrections are not large; viz., $\langle \cos(\theta) \rangle = 0.895$ and 0.903 and $\langle v/c \rangle = 0.977$ and 0.968 for the ground and 1.27-MeV transitions, respectively.

We gather the systematic uncertainties, expressed in terms of the ratio $\mathcal{A}_{g.s.}/\mathcal{A}_{ex}$, in Table I. No correction for these possible systematic effects was applied to the experimentally determined ratio, and there is no evidence that these effects will preferentially increase or decrease the measured ratio.

E. Numerical example of the analysis

Although small portions of the data set were examined for time-dependent and systematic effects, the data were eventually grouped into five statistically significant groups. Within each group, the beam polarization, target orientation, and magnetic-holding field orientation were constant. The numerical evaluations of the ground- and excited-state asymmetries for one group, as various corrections were applied, are given in Tables II and III, respectively. Because the background corrections are large and in general time dependent, the results for the three separate measurement intervals are given for the transition to the 1.27-MeV level in ^{29}Si . A fit to the time dependence of the 1.78-MeV Si γ -ray corrected asymmetry (last column of Table III) using the relaxation time $T_1 = 11.2$ s obtained from the ground-state transition (see Fig. 2) gives $\chi^2 = 1.2$ for two degrees of freedom. The significant background subtractions increase the excited-state asymmetry by a factor of 3. Similar results were obtained for the other four groups.

V. RESULTS AND DISCUSSION

A. Results

The ratio $\mathcal{A}_{g.s.}/\mathcal{A}_{ex}$ for each of the five data sets is given in Table IV. The weighted mean is -2.042 with a statistical uncertainty of ± 0.233 . The χ -squared per degree of freedom (χ^2/ν) is 0.84. When combined with the systematic error of ± 0.110 from Table I, the final result is $\mathcal{A}_{g.s.}/\mathcal{A}_{ex} = -2.04 \pm 0.26$.

TABLE III. Evolution of the asymmetry for 1.27-MeV photopeak region of the γ -ray spectrum as corrections are made to obtain \mathcal{A}_{ex} for ^{29}P decay to the 1.27-MeV first excited state in ^{29}Si . These data are from the fourth measurement, and are given for the three measuring intervals of 2, 2, and 4 s (labeled T1–T3, respectively). The final results are corrected for averaging $\cos(\theta)$ over the beta detector solid angle and v/c over the beta spectrum using the cut shown in Fig. 3.

1.27-MeV transition	Measurement interval	Percent of the events	Measurement asymmetry $\times 100$	Corrected asymmetry $\times 100$
Cut 1.27-MeV γ ray	T1	34.15 \pm 0.09	–0.33 \pm 0.19	
	T2	27.19 \pm 0.08	–0.51 \pm 0.21	
	T3	38.66 \pm 0.10	–0.14 \pm 0.18	
Accidentals and pileup	T1	1.57 \pm 0.02	2.38 \pm 0.54	–0.45 \pm 0.20
	T2	1.05 \pm 0.01	2.75 \pm 0.65	–0.64 \pm 0.22
	T3	1.25 \pm 0.01	1.23 \pm 0.59	–0.19 \pm 0.19
Annihilation in flight	T1	3.60 \pm 0.03	2.57 \pm 0.01	–0.83 \pm 0.25
	T2	2.88 \pm 0.02	2.10 \pm 0.01	–0.96 \pm 0.27
	T3	4.09 \pm 0.03	1.64 \pm 0.01	–0.38 \pm 0.22
1.78-MeV ^{28}Si γ ray	T1	3.74 \pm 0.04	–0.16 \pm 0.43	–0.93 \pm 0.29
	T2	3.95 \pm 0.04	0.09 \pm 0.40	–1.17 \pm 0.33
	T3	8.78 \pm 0.06	0.02 \pm 0.28	–0.51 \pm 0.31
Final result		69.08 \pm 0.12		–0.94 \pm 0.19

Naviliat-Cuncic *et al.*²³ have recently compiled the $\mathcal{F}t$ values and made predictions of the asymmetry parameter $A_{\mathcal{F}t}$ for all mirror transitions in the $1p$ and $2s\ 1d$ shells. Their calculations include the revised^{5,6} radiative correction terms and isospin nonconservation corrections²⁴ similar to those employed elsewhere.^{1,3,5} Detailed calculations of the isospin corrections, such as those performed by Ormand and Brown⁴ for superallowed transitions, are generally not available for these mirror transitions. Likewise, reliable estimates of the recoil order corrections are also lacking for many of the transitions. However, these remaining corrections are believed to be small,^{1,7,23} corresponding to a $\lesssim 0.3\%$ and $\lesssim 1\%$ change in $A_{\mathcal{F}t}$ for the isospin and recoil corrections, respectively. Equation (8) can be evaluated using $A_{\text{ex}} = -\frac{1}{3}$, the Naviliat-Cuncic *et al.* asymmetry parameter for ^{29}P , $A_{\mathcal{F}t} = -0.6061 \pm 0.0044$, and the measured ratio $\mathcal{A}_{\text{g.s.}}/\mathcal{A}_{\text{ex}} = -2.04 \pm 0.26$. The result

$$\left(\frac{A_{\text{ex}}}{A_{\mathcal{F}t}} \right) \left(\frac{\mathcal{A}_{\text{g.s.}}}{\mathcal{A}_{\text{ex}}} \right) = 1.12 \pm 0.14, \quad (9)$$

TABLE IV. Results from five separate measurements of $\mathcal{A}_{\text{g.s.}}/\mathcal{A}_{\text{ex}}$. The χ -squared per degree of freedom (χ^2/ν) about the weighted mean is 0.84. The systematic error contribution is taken from Table I.

Measurement	$\mathcal{A}_{\text{g.s.}}/\mathcal{A}_{\text{ex}}$	
1	–2.491 \pm 1.226	
2	–1.621 \pm 0.540	
3	–1.803 \pm 0.344	
4	–2.659 \pm 0.538	
5	–2.688 \pm 0.733	
Weighted mean	–2.042 \pm 0.233	$\chi^2/\nu = 0.84$
Systematic error	± 0.110	
Final result	–2.04 \pm 0.26	

is in agreement with the expected value of unity. Assuming that the calculation of A_{ex} and the real asymmetry parameter for the excited state are equal, the experimental value for the mirror transition asymmetry parameter is $A_{\text{g.s.}} = 0.681 \pm 0.086$.

B. Comparison with other mirror transitions

The results for the five mirror transitions investigated so far are collected in Table V, and the ratio $\mathcal{R} = A_{\text{exp}}/A_{\mathcal{F}t}$ for these transitions is shown in Fig. 6. The statistical factor \mathcal{F} for the neutron is very well deter-

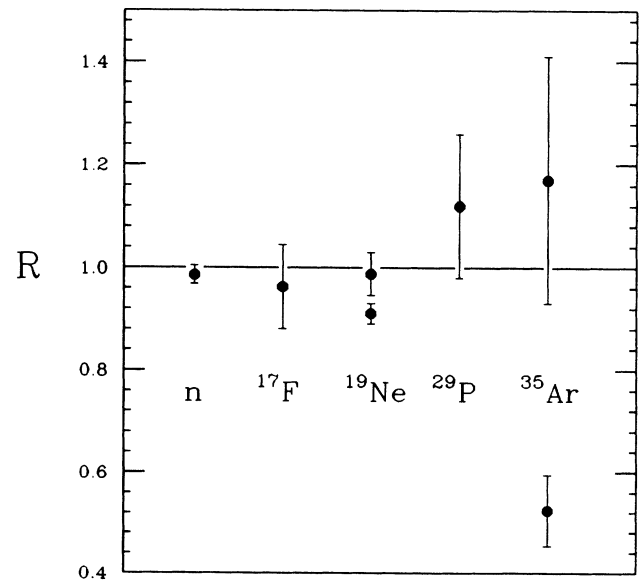


FIG. 6. The ratio $\mathcal{R} = A_{\text{exp}}/A_{\mathcal{F}t}$ for the five mirror transitions studied to date. The numerical values are given in Table V.

TABLE V. Results of $\mathcal{F}t$ calculations, asymmetry parameter $A_{\mathcal{F}t}$ calculations, asymmetry parameter A_{exp} measurements, and the ratios $\mathcal{R} = A_{\text{exp}}/A_{\mathcal{F}t}$ for the five mirror transitions studied to date. Recoil order corrections are in general not included. See the text for details.

Nucleus	$\mathcal{F}t^a$	$A_{\mathcal{F}t}$	A_{exp}	$\mathcal{R} = A_{\text{exp}}/A_{\mathcal{F}t}$
n	1056.3 ± 3.1^b	-0.11623 ± 0.00085	-0.1146 ± 0.0019^c	0.986 ± 0.018
^{17}F	2314.0 ± 6.9	0.99715 ± 0.00016	0.960 ± 0.082^d	0.962 ± 0.082
^{19}Ne	1725.1 ± 4.4	-0.03957 ± 0.00089	-0.0391 ± 0.0014^e	0.988 ± 0.042
^{19}Ne	1726.8 ± 0.4^f	-0.03991 ± 0.00016	-0.0363 ± 0.0008^g	0.910 ± 0.020
^{20}P	4869.1 ± 18.1	0.6061 ± 0.0044	0.681 ± 0.086^h	1.12 ± 0.14
^{35}Ar	5717.7 ± 14.2	0.4201 ± 0.0071	0.49 ± 0.10^i	1.17 ± 0.24
^{35}Ar			0.22 ± 0.03^j	0.524 ± 0.071

^aUnless otherwise noted, $\mathcal{F}t$ values are from Ref. 23.

^bReference 10.

^cReference 9.

^dReference 12.

^eReference 25.

^fThe half-life was taken from Ref. 27.

^gReference 26.

^hThe present work.

ⁱReference 11.

^jFrom the analysis of Ref. 16.

mined,¹ and the recoil order corrections^{7,9} are small because of the low transition energy. For ^{19}Ne the recoil order corrections to \mathcal{R} are again negligible because the experimental value for the asymmetry parameter results from an extrapolation^{25,26} to zero energy. Thus the shortcomings in the analysis by Naviliat-Cuncic *et al.* do not limit the accuracy with which the experimentally determined asymmetry parameter can be compared to $A_{\mathcal{F}t}$.

With the exception of the most recent, unpublished results^{26,27} for ^{19}Ne and the early results for ^{35}Ar decay that were analyzed by Hardy and Towner,¹⁶ all transitions are in good agreement with the usual assumptions of the $V-A$ theory of nuclear beta decay. The ^{19}Ne disagreement was originally pointed out by Deutsch,⁸ and should not be considered seriously until it is confirmed. The anomalous ^{35}Ar result is in disagreement with the recent measurement of Garnett *et al.*,¹¹ and speculations as to the origin of this apparent violation of CVC have also been laid to rest.²⁸ In principle the ^{24}Al result²⁸ could be included in an analysis of the mirror transitions, but Adelberger *et al.*²⁸ argue persuasively that this is a pure Fermi transition, and as such it should be treated on an equal footing with other superallowed decays.

C. Future directions

In general the anticipated deviations from $V-A$ are much smaller than the uncertainties in \mathcal{R} given in Table V. For example, recoil order and, perhaps, unexpected isospin nonconservation contributions probably will enter only at the level of $<0.5\%$, and will be much smaller for neutron decay. Exotic contributions, such as from a mas-

sive right-handed gauge boson in left-right symmetric theories,⁸ are limited to a similar level for semileptonic decays. There are exceptions, however. For example, the neutron and ^{19}Ne decays exhibit enhanced sensitivity to the left-right mixing angle (approximately 2% and 6% in \mathcal{R} at the present semileptonic limits, respectively), but constraints from purely leptonic muon decay and unitarity are quite restrictive⁸ and should apply to semileptonic decays also.

The difficulty encountered with producing polarized nuclei by polarization transfer reactions is that the polarizations achieved are typically quite small, and the final error scales roughly as $1/P$. The low-temperature "brute force" polarization technique¹² is more promising in this respect, but it is encumbered by an approximately 2% systematic uncertainty in the polarization. This uncertainty can in principle be reduced by using the excited-state ratio method employed here, but the activities presently achievable are far too meager for such an experiment. Optical pumping techniques²⁹ are also potentially promising, but have yet to be successfully applied to decays of interest. Therefore achieving a significant asymmetry parameter test of the $V-A$ theory in mirror transitions, even at the level of the recoil order contributions, will be quite difficult.

ACKNOWLEDGMENTS

We would like to thank Doctor S. J. Freedman for suggesting this experiment and for providing some of the beta detectors. This work was supported in part by the U.S. National Science Foundation under Grant No. PHY-8717764.

*Present address: Department of Physics, University of Basel, Klingelbergstrasse 82, CH 4056, Basel, Switzerland.

¹D. H. Wilkinson, in *Nuclear Weak Processes and Nuclear Structure*, edited by M. Morita, H. Ejiri, H. Ohtsubo, and T. Sato (World Scientific, Singapore, 1989), p. 1.

²V. T. Koslowsky, E. Hagberg, J. C. Hardy, H. Schmeing, R. E. Azuma, and I. S. Towner, in *Proceedings of the 7th International Conference on Atomic Masses and Fundamental Constants, 1984*, edited by O. Klepper (Gesellschaft für Schwerionenforschung, Darmstadt, 1984), p. 572; I. S. Town-

- er and J. C. Hardy, *ibid.*, p. 564.
- ³J. C. Hardy, I. S. Towner, V. T. Koslowsky, E. Hagberg, and H. Schmeing, Nucl. Phys. **A509**, 429 (1990).
- ⁴W. E. Ormand and B. A. Brown, Phys. Rev. Lett. **62**, 866 (1989); **63**, 103 (1989).
- ⁵A. Sirlin and R. Zucchini, Phys. Rev. Lett. **57**, 1994 (1986).
- ⁶W. Jaus and G. Rasche, Phys. Rev. D **35**, 3420 (1987); A. Sirlin, Phys. Rev. D **35**, 3423 (1987).
- ⁷B. R. Holstein, Rev. Mod. Phys. **46**, 789 (1974); **48**, 673 (1976).
- ⁸J. Deutsch, in *Fundamental Symmetries and Nuclear Structure*, edited by J. N. Ginocchio and S. P. Rosen (World Scientific, Singapore, 1989), p. 36.
- ⁹E. Klemt, P. Bopp, L. Hornig, J. Last, S. J. Freedman, D. Dubbers, and O. Schärpf, Z. Phys. C **37**, 179 (1988).
- ¹⁰W. Mampe, P. Agreron, C. Bates, J. M. Pendelbury, and A. Steyerl, Phys. Rev. Lett. **63**, 593 (1989).
- ¹¹J. D. Garnett, E. D. Commins, K. T. Lesko, and E. B. Norman, Phys. Rev. Lett. **60**, 499 (1988).
- ¹²N. Severijns, J. Wouters, J. Vanhaverbeke, and L. Vanneste, Phys. Rev. Lett. **63**, 1050 (1989).
- ¹³J. C. Hardy and I. S. Towner, Nucl. Phys. **A254**, 221 (1975); W. E. Ormand, B. A. Brown, and B. R. Holstein, Phys. Rev. C **40**, 2914 (1989).
- ¹⁴D. H. Wilkinson and B. E. F. Macefield, Nucl. Phys. **A232**, 58 (1974).
- ¹⁵W. C. Mead, Ph.D. dissertation, Princeton University, 1973.
- ¹⁶J. C. Hardy and I. S. Towner, Phys. Lett. **58B**, 261 (1975).
- ¹⁷G. Azuelos and J. E. Kitching, Nucl. Phys. **A285**, 19 (1977).
- ¹⁸W. Haeberli, M. D. Barker, C. A. Gossett, D. G. Mavis, P. A. Quin, J. Sowinski, T. Wise, and H. F. Glavish, Nucl. Instrum. Methods **196**, 319 (1982).
- ¹⁹P. M. Endt and C. van der Leun, Nucl. Phys. **A310**, 1 (1978).
- ²⁰Wang Zhenjie, R. A. Bigelow, P. A. Quin, and J. Liechti, Phys. Rev. C **40**, 1586 (1989).
- ²¹J. B. Gerhart, B. C. Calson, and R. Scherr, Phys. Rev. **4**, 917 (1954).
- ²²W. Haeberli (private communication); V. J. Zeps, Ph.D. dissertation, University of Washington, 1989.
- ²³O. Naviliat-Cuncic, T. A. Girard, N. Severijns, and J. Deutsch (unpublished).
- ²⁴S. Raman, C. A. Houser, T. A. Walkiewicz, and I. S. Towner, At. Data Nucl. Data Tables **21**, 567 (1978).
- ²⁵F. P. Calaprice, S. J. Freedman, W. C. Mead, and H. C. Vantine, Phys. Rev. Lett. **35**, 1566 (1975).
- ²⁶D. F. Schreiber, Ph.D. dissertation, Princeton University, 1983.
- ²⁷L. E. Piilonen, Ph.D. dissertation, Princeton University, 1985.
- ²⁸E. G. Adelberger, P. B. Fernandez, C. A. Gossett, J. L. Osborne, and V. J. Zeps, Phys. Rev. Lett. **55**, 2129 (1985).
- ²⁹M. Kitano, M. Bourzutschky, F. P. Calaprice, J. Crayhold, W. Happer, and M. Mushhoff, Phys. Rev. C **34**, 1974 (1986).